MASSACHUSETTS INSTITUTE OF TECHNOLOGY
ARTIFICIAL INTELLIGENCE LABORATORY

A.I. Memo No. 1262 October 1990

Contact Sensing from Force Measurements

Antonio Bicchi
J. Kenneth Salisbury
David L. Brock

Abstract

This paper addresses contact sensing, i.e. the problem of resolving the location of a contact, the force at the interface and the moment about the contact normals. Called "intrinsic" contact sensing for the use of internal force and torque measurements, this method allows for practical devices which provide simple, relevant contact information in practical robotic applications. Such sensors have been used in conjunction with robot hands to identify objects, determine surface friction, detect slip, augment grasp stability, measure object mass, probe surfaces, control collision and a variety of other useful tasks. This paper describes the theoretical basis for their operation and provides a framework for future device design.

This report describes research performed at the Artificial Intelligence Laboratory of the Massachusetts Institute of Technology. Support for this research is provided by the University Research Initiative Program under Office of Naval Research contract N00014-86-K-0685, NASA contract number NAG-9-319 and the Progetto Finalizzato Robotica, CNR. Antonio Bicchi is a Research Associate on leave from DSEA, Dipartimento di Sistemi Elettrici e di Automazione, Università di Pisa, Pisa, Italy. Support for Antonio Bicchi as a Visiting Scientist at the Artificial Intelligence Laboratory has been provided by a NATO-CNR joint fellowship program, grant No. 215.22/07.

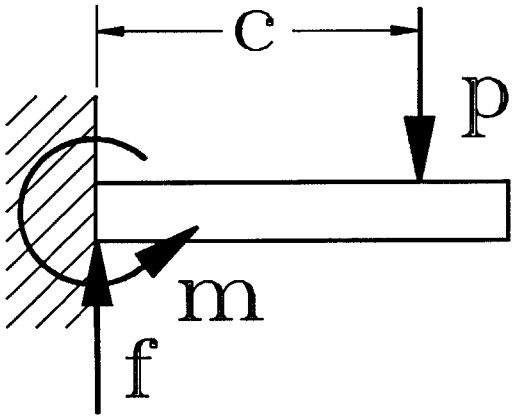

Figure 1: Simple contact sensing.

1 Introduction

Manipulation requires contact between a robot and an object. Although contact is the fundamental interaction which occurs in manipulation, most robotic systems rely on a priori positional information in order to perform tasks. Current robot systems do not adequately sense or use contact information. Instead, they rely on precise pre-positioned objects and arm joint information to guide the robot into contact with these objects. When contact occurs, as in grasping and assembly operations, more precise and intrinsically mechanical information is required than can be obtained from vision or non-contact sensing. The traditional approach to monitoring and controlling such interactions falls into two camps: force sensing and tactile sensing. The "classic" approach to force sensing employs strain sensitive elements in the wrist, drive train and other arm structures to permit measurement and control of contact and assembly forces (see Whitney [1987] for an overview). This method focuses on the net contact force and does not address contact location and geometry. On the other extreme, tactile sensors have been used to sense the details of particular contacts. Such devices employ surface mounted arrays of force sensitive elements which can be used to reveal contact locations, shapes and contact pressure distributions. See Nicholls and Lee [1989] for an extensive survey of the technology.

An alternative approach to traditional force and tactile sensing, developed in detail here, relies on the use of force and torque measurements to reveal a contact's location and force components. One of the simplest embodiments of this concept is shown in figure 1.

By measuring the moment m and the force f at the fixed end of the cantilever beam, both the position of a single contact and the magnitude of its normal component of force can be found as: $p = f$ and $c = m/f$. A two-dimensional version of this idea permits contact

location and normal force measurement on a plane by simply measuring the force normal to the plane and two moments in the plane. One embodiment of this idea was patented by Peronneau [1972]. It turns out that it is also possible to sense the location and force components of contacts occurring on a non-planar body, under appropriate assumptions. Minsky [1972] mentions this idea in conjunction with a force sensing wrist on a robot.

Salisbury [1984] and Brock and Chiu [1985] described a structural and mathematical solution appropriate for robot fingertips that sense the location of point contacts which transmit pure forces, along with the components of the contact forces themselves. Their approach has been reconsidered by Tsujimura and Yabuta [1988]. Okada [1990] presented a suspension-cell based tactile sensor, very close in spirit to this sensing concept. Bicchi [1989, 1990a] derived a complete solution which takes into account soft-finger contact effects. Eberman and Salisbury [1989] describe how joint torque measurements in a robot arm may be used to determine the location of a contact on its links. The broad applicability of this concept warrants closer examination of the underlying mathematics and has thus motivated this paper.

This type of force-based contact sensing is inherently different from more traditional tactile sensing. The goal of most tactile sensing systems is to measure the pressure distribution over the area of contact in order to infer details about contact location and shape. However, the goal of force-based contact sensing is to measure the net force acting on a body and to use this data to determine the properties of the contact through which the force is exerted. Since these sensors rely on measurements taken by sensing elements which are placed inside, rather than spread over, the contacting surface, they are also referred to as intrinsic tactile sensors.

Although the theory behind such sensors is relatively complex, in practice they are quite simple to build and utilize, and therefore offer enormous potential for improving robot manipulation dexterity. In this paper we present the theoretical aspects of intrinsic contact sensing as a basis for device design and application. In section 2, we survey three basic contact models: the *point contact without friction*, *point contact with friction* and *soft finger contact*. The soft finger contact type is particularly important, since it describes the most common situation encountered in manipulation. In section 3, we address the basic mathematics and mechanics of contact sensing, and discuss when it is possible for a sensor to determine the location and the resultant force and moment of a contact given internal force and moment measurements. Sections 4, 5, and 6 describe algorithms to solve the contact sensing problem: section 4 presents a general, yet approximate, closed-form algorithm, section 5 describes a closed-form, exact solution for a number of simple sensor surfaces, and section 6 introduces a general iterative method. Section 7 describes some possible generalizations of the idea; finally, in section 8 numerical experiments are used to discuss the properties of the proposed algorithms. The appendix contains proofs of the propositions introduced in the text.

2 Contact Types

The concept of contact *type* is basic to understanding force-based contact sensing. The contact type establishes constraints on the forces which may be applied through the contact between two bodies [Mason and Salisbury, 1985].

If the forces which act upon a body sum to zero, it is said to be in a state of static equilibrium. These forces may arise from actuators, body forces and contacts with the environment. Although the net force and moment on a system in static equilibrium will sum to zero, there will be non-zero internal forces (i.e. structural stresses, contact forces etc.). If measurements of some of the internal forces can be made, they can be checked for consistency with the expected effects of a particular load type, and hence can be used to deduce information about the contact(s).

In the case of a body in contact with another when arbitrary forces and moments can be transmitted through the contact (i.e. a *glued contact* type), not much may be said about the contact geometry, starting from force measurements. However, other common contact types impose constraints on the transmitted forces: their components usually have to be either unidirectional or limited by friction cones. It is these constraints which make the whole concept practical.

A *point contact without friction* constrains the force applied to the body to be normal to the surface at the point of contact, and the moment to be zero. There are only 3 unknowns, the 2 contact coordinates on the surface and the force magnitude, so ideally only 3 independent force measurements would be required to reveal the contact location and force. If we precisely measure all 3 force components acting on the body, the associated wrench axis is a line which passes through the point of contact and is normal to the surface at that contact point [1].

A *point contact with friction* also constrains the force applied to the body to be a pure force, but it is no longer constrained to have a line of action normal to the surface at the point of contact (it must however lie within the friction cone at the point of contact). Since there are now 5 unknowns, the 2 contact coordinates and the 3 contact force components, ideally only 5 independent force measurements are required to measure the contact location and force components. Again, if precise measurements are available, the associated wrench axis is a line which passes through the point of contact.

Finally, if due to the compliance of the bodies, finite portions of the surface come into contact, and if friction is present, torques may also be exerted on the body. In this situation, often referred to as *soft finger contact*, the wrench axis no longer necessarily passes through the contact location. As will be shown below it is possible to define and solve for the contact location, and force and moment components even in this rather general case.

[1] The *wrench axis* is a generalization of the concept of line of action of forces acting on a body. When an arbitrary set of forces and torques acts on a body, they may be canonically described by a unique line in space along which a unique force acts, and parallel to which a unique moment acts (see [Hunt, 1978]).

2.1 Soft Finger Contact and the Contact Centroid

The soft finger type of contact is the most general case, among those considered above, to which intrinsic contact sensing can be applied. Point contacts with or without friction are particular cases of soft finger contacts. Indeed, this type of contact is also the most common in practical manipulation: for instance, contacts through which humans and rubber covered robot hands manipulate objects are frequently of this type.

A soft finger contact occurs between two real (non-rigid, possibly inelastic) bodies mutually transmitting a distribution of contact tractions[2] over a finite area of contact. The tractions are assumed to be *compressive*, that is, to point at the interior part of the body (adhesive forces between bodies are therefore disregarded by this model). Because of their distributed nature, a complete characterization of contact related phenomena would involve complex continuum mechanics relationships, whose computation (if at all possible) is far beyond the capabilities and needs of a real-time robot sensory and control system. A compact characterization of contact is necessary to render the sensing problem tractable. The traditional approach to tactile sensing consists of spatially sampling the traction distribution, and is usually limited to sensing only normal force components. A more drastic compression of data is obtained by force-based contact sensing, which provides a reduced set of contact features, useful for manipulation control. This is achieved by the use of an *equivalent set* of forces. Roughly speaking, two sets of forces are equivalent if their large-scale effects are the same. The unknown distribution of contact tractions can be substituted with an equivalent set of forces, comprised only of a *resultant force* (henceforth designated by the vector $\mathbf{p}$), and a *resultant moment*, $\mathbf{q}$. Finally, to completely describe the set of forces, also a point must be provided, through which the resultant force effectively is applied. The choice of this point is not trivial in the soft finger case, because contact occurs over a whole area. We show in what follows that a very convenient point to use for representing soft finger contacts is the *contact centroid*, which we define as follows:

Definition of Contact Centroid

Given a surface S with an outward normal direction defined everywhere on it, and a distribution Δ of compressive tractions applied on it, a contact centroid for S and Δ is a point on S such that a set of forces equivalent to Δ exists, having the following characteristics:

i) it is comprised of only a force and a torque;

ii) the force $\mathbf{p}$ is applied at that point, and is directed into S;

iii) the moment $\mathbf{q}$ is parallel to the surface normal at that point (i.e. a pure torque about the contact normal).

[2]The term *traction* [Johnson,1985] indicates a force per surface unit, comprised in general of a normal component (pressure) and tangential (friction) components.

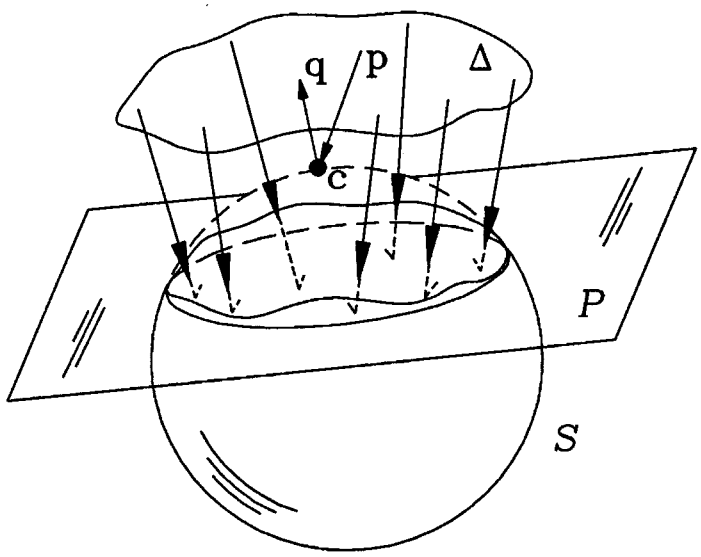

Figure 2: The contact centroid has the property of being close to the actual contact area.

A contact centroid *per se* has some very useful properties that render it a desirable point to sense. Firstly, if contact occurs at a single point, a contact centroid coincides with that point. Thus, from force/torque measurements we can obtain geometric information about where the contact occurs, a typical tactile sensing goal. Useful geometric information is still contained in the contact centroid even when multiple points and/or finite areas are in contact. In fact, a contact centroid has an important property, which can be articulated as follows:

Proposition 1: Property of Contact Centroids

Consider a deformable body, whose undeformed surface S is convex, and assume that a distribution Δ of compressive contact tractions is exerted on it. Consider a plane P that divides the surface of the body in two portions, confining every contact point to one half-space (see figure 2). Consider the projection of each contact point onto P along the direction of the traction applied at the contact point itself: if all such projected points lie within the volume surrounded by the undeformed surface S, then the contact centroid [3] lies on the same side of P where Δ is applied.

The proof of this property takes a few steps, and is presented in Appendix 1. The significance of this property is related to the fact (to be proved shortly) that it is possible

[3]We will show in section 3 that for convex surfaces the contact centroid is actually unique

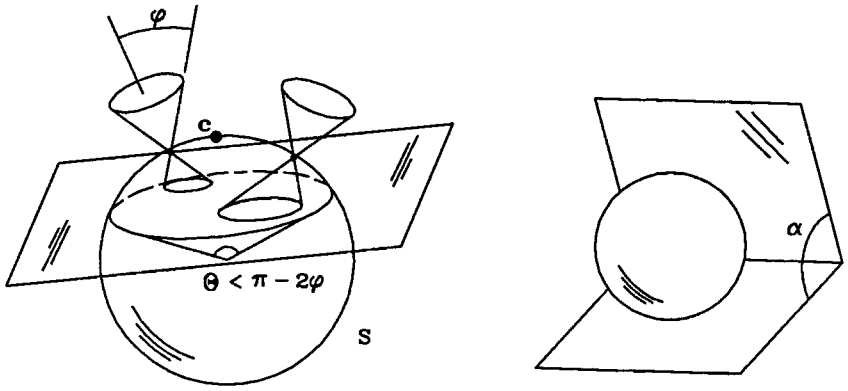

Figure 3: A spherical sensor surface with friction coefficient $\mu = \tan\varphi$.

to give an expression of the contact centroid in terms of force/torque measurements only. Accordingly, although an intrinsic contact sensor is not able to provide an *image* of the actual contact points, if some hypothesis on curvature, deformability and friction of the surface are satisfied, we have at least an idea about the location of contact points over the sensor surface, since they are constrained to lie "near" the contact centroid[4] (see figure 2).

As a corollary to the property above, let us consider a generic compressive distribution Δ, whose tractions comply with Coulomb's friction law. According to the above assumptions, it is required that the intersections with P of every friction cone lie inside the volume surrounded by S. Consider for instance a spherical sensor surface, with coefficient of friction $\mu = \tan\varphi$ and small deformability (see figure 3). It can be easily shown that the hypotheses of the above property apply in this case if every contact point can be seen from the center of the sphere within an angle $\theta = \pi - 2\varphi$. In other words, if the contact area warped around the surface is "small" enough (and this bound can be quantified), then the contact centroid is a valid datum about contact. For a cylindrical or spherical sensor wedged in a corner with angle α, and friction angle φ, the condition is $\alpha > 2\ \varphi$.

[4]The concept of contact centroid was not explicit in the initial definition of soft finger contact given by Salisbury [1982], that was based on an assumption of very small contact area. The contact centroid introduced by Bicchi[1989] allows for a broader applicability of the soft finger contact type. It should be further noted that, for flat surfaces, the contact centroid coincides with the center of friction introduced by Mason [Mason and Salisbury, 1985].

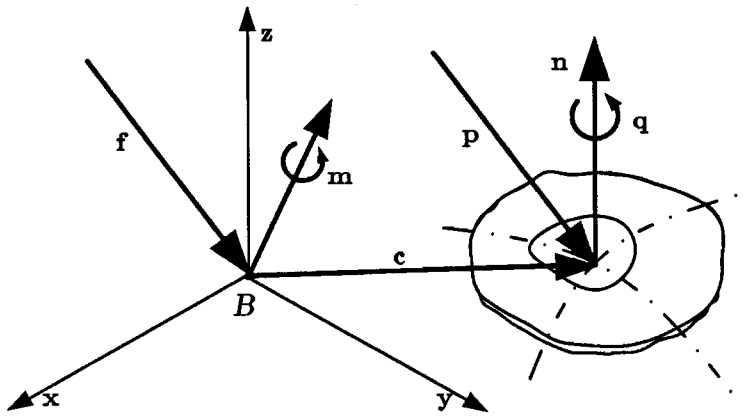

Figure 4: Vector quantities and notation involved in the problem statement.

3 Problem Formulation

One possible implementation of an intrinsic contact sensor consists of a surface, which we will call a *fingertip*, supported by a six-axis force/torque sensor. The force/torque sensor measures all three components of both the resultant force $\mathbf{f}$ and the resultant moment $\mathbf{m}$ with respect to the reference frame B, as shown in figure 4. Note that the choice of the reference frame B is arbitrary, since we can easily express $\mathbf{f}$ and $\mathbf{m}$ in terms of any other coordinate frame fixed to B.

The fingertip surface can be described by the implicit relation

$$S(\mathbf{r}) = 0, \tag{1}$$

where $\mathbf{r}$ is a point in space defined with respect to B. The surface S should have continuous first derivatives, so that a normal unit vector can be defined at every point on S as

$$\mathbf{n} = \frac{\nabla S(\mathbf{r})}{||\nabla S(\mathbf{r})||},$$

where ∇ indicates the gradient operator. Let $\mathbf{c}$ be the contact centroid, and $\mathbf{p}$, $\mathbf{q}$ the force and moment applied at $\mathbf{c}$, which are equivalent to a "soft finger" contact. The measurable quantities $\mathbf{f}$ and $\mathbf{m}$ are related to the unknowns $\mathbf{c}$, $\mathbf{p}$ and $\mathbf{q}$, by force and moment balance equations,

$$\mathbf{f} = \mathbf{p}, \tag{2}$$

$$\mathbf{m} = \mathbf{q} + \mathbf{c} \times \mathbf{p}. \tag{3}$$

For soft finger contacts the torque $\mathbf{q}$ is parallel to the unit vector $\mathbf{n}$ normal to the surface at the contact centroid $\mathbf{c}$, hence

$$\mathbf{n} \propto \mathbf{q} = \frac{K}{2} \nabla S(\mathbf{c}), \tag{4}$$

for some constant K.

We call the above set of relations the *contact sensing problem*:

> Given the measurements $\mathbf{f}$ and $\mathbf{m}$, along with a surface equation $S(\cdot) = 0$, determine the location of the contact centroid(s) $\mathbf{c}$, and the related contact force $\mathbf{p}$ and moment(s) $\mathbf{q}$.

Note that, because of the definition of contact centroid, we implicitly require that $\mathbf{p}$ is compressive, i.e. directed into the surface, and that $\mathbf{q}$ is normal to S. Expanding equations 1 through 4 yields a non-linear system of ten equations in ten scalar unknowns, i.e. the nine components of $\mathbf{p}$, $\mathbf{q}$, $\mathbf{c}$, and K. However, by simply substituting equations 2 and 4 in equation 3, the problem is reduced to four equations in four unknowns. Since the problem is non-linear, we need to determine if a solution exists, and in that case if it is unique.

In general, not much can be said about the existence of solutions: given arbitrary $\mathbf{f}$, $\mathbf{m}$, and S, there is no guarantee we can find an equivalent soft finger contact. A solution exists, however, if the resultant force $\mathbf{f}$ and and moment $\mathbf{m}$ are measurements consistent with the effects of a soft-finger type traction distribution on S.

If a solution exists, the following proposition holds about its uniqueness:

> **Proposition 2: Uniqueness of Solutions**
>
> A solution to the contact sensing problem is unique (if it exists), if and only if the sensor surface is convex (see proof in Appendix 2).

Proposition 1 gives conditions on Δ and S that guarantee the existence of a contact centroid. According to proposition 2, the contact centroid of a compressive distribution Δ on a convex surface is also unique.

As a final remark, the solution to equations 1 through 4 may not be trivial and a closed-form solution may not be found except for the simplest surfaces. In the following sections, we will present three methods for solving these equations: first the simple point contact solution , next the ellipsoidal solution and finally a general iterative solution.

4 Point-contact solution

The first closed-form method we present for solving the contact sensing problem utilizes more restrictive assumptions than those specified in the following sections. In particular, we assume the local torque $\mathbf{q}$ about the contact normal is zero. In other words we assume the

contact model is a *point contact with friction*, as described in section 2. This assumption can lead to good results and a simple solution for a large number of practical cases. The *wrench axis* of the force system is given by

$$\mathbf{r} = \mathbf{r}_0 + \lambda \mathbf{f}, \tag{5}$$

where

$$\mathbf{r}_0 = \frac{\mathbf{f} \times \mathbf{m}}{\|\mathbf{f}\|^2}. \tag{6}$$

The wrench axis is a line through $\mathbf{r}_0$ and parallel to $\mathbf{f}$, parameterized by λ. This line intersects the convex surface S in at most two locations: one corresponding to a force pulling out of the surface and one corresponding to a force pushing into the surface. Since we do not allow adhesive forces, we can determine the contact centroid as the intersection point, for which the contact force is directed into the surface, that is

$$\mathbf{f}^T \mathbf{n}(\mathbf{c}) < 0. \tag{7}$$

When the local torque $\mathbf{q}$ is not zero, the point found by this method differs from the contact centroid. Therefore we will denote with $\mathbf{c}'$ the vector found using this (so-called "wrench-axis" or "point-contact") method.

Note that the assumption $\mathbf{q} = 0$ can be checked out directly from force/torque measurements by means of the equivalent relationship $\mathbf{f}^T \mathbf{m} = 0$. We should point out that the point $\mathbf{c}'$ does not have any of the properties of contact centroids, so that it could in principle lie far away from the actual location of the contact area. Yet, point $\mathbf{c}'$ retains a valuable meaning in real conditions as an easy-to-compute approximation of the contact centroid. In order to give an estimate of the distance between $\mathbf{c}'$ and the contact centroid $\mathbf{c}$, let $\mathbf{e}$ represent the difference vector $\mathbf{e} = \mathbf{c}' - \mathbf{c}$. The two sets of forces and torques, $\mathbf{p}$, $\mathbf{q}$ applied at $\mathbf{c}$, and $\mathbf{p}$, $\mathbf{t}$ applied at $\mathbf{c}'$, are both equivalent with the actual set of contact forces, hence they are equivalent with each other. The balance equation of moments about $\mathbf{c}$ can be written as

$$\mathbf{q} = \mathbf{t} + \mathbf{e} \times \mathbf{p}.$$

Such a vector equation is solved by any $\mathbf{e}$ of the form

$$\mathbf{e} = \frac{(\mathbf{q} - \mathbf{t}) \times \mathbf{p}}{\|\mathbf{p}\|^2} + \nu \mathbf{p}. \tag{8}$$

Recalling that, from the definition of wrench axis, $\mathbf{t}$ is parallel to $\mathbf{p}$, and that, by the definition of contact centroid, $\mathbf{q}$ is normal to the surface, we can rewrite equation 8 as

$$\mathbf{e} = \frac{\mathbf{q} \times \mathbf{p}_t}{\|\mathbf{p}\|^2} + \nu \mathbf{p},$$

where $\mathbf{p}_t = \mathbf{p} - (\mathbf{p}^T\mathbf{n})\mathbf{n}$ is the tangential (friction) component of the contact resultant force. Since the error vector $\mathbf{e}$ is the sum of two mutually orthogonal vectors, its length is at least as large as:

$$\|\mathbf{e}\| \geq \frac{\|\mathbf{q}\| \, \|\mathbf{p}_t\|}{\|\mathbf{p}\|^2}.$$

In view of this result, it can be observed that, when the local torque $\mathbf{q}$ is not zero, the distance between the point found by the wrench-axis method and the contact centroid grows quickly as friction increases. Thus, the approximation of the contact centroid with point $\mathbf{c}'$ should be avoided if high-friction and/or compliant materials are employed in building the fingertips. Numerical examples are provided in the discussion section.

5 Solution for Ellipsoidal Surfaces

The main advantage of the wrench-axis method is that the contact location problem is reduced to that of finding the intersections of a line with a surface, that is, to elementary geometry. However, this method has two major drawbacks: first, it does not provide information about the moment exerted through a soft-finger contact, and second, it only approximates the contact centroid when $\mathbf{q}$ is not zero. In this section we solve the contact sensing problem and avoid such shortcomings. However, in order to guarantee a closed-form algorithm and to simplify calculations, the fingertip surface will be restricted to belong to a specific class of surfaces, namely, quadratic forms of the type

$$S(\mathbf{r}) = \mathbf{r}^T\mathbf{A}^T\mathbf{A}\mathbf{r} - R^2 = 0, \tag{9}$$

where $\mathbf{A}$ is a constant coefficient matrix, and R is a scale factor used for convenience. Since the reference frame B can be moved arbitrarily, we can assume without loss of generality that $\mathbf{A}$ can be written in diagonal form

$$\mathbf{A} = \begin{pmatrix} 1/\alpha & 0 & 0 \\ 0 & 1/\beta & 0 \\ 0 & 0 & 1/\gamma \end{pmatrix}.$$

In order to guarantee the uniqueness of solutions, the surface specification must be further restricted to convex portions of the quadratic form (for instance, one of the sheets of a double hyperboloid would be an appropriate sensor surface). In the interest of simplicity, however, we will consider in the following only general ellipsoids (i.e., positive definite $\mathbf{A}$ matrices). In this case, the principal axes of the ellipsoid are given by $2\alpha R$, $2\beta R$ and $2\gamma R$, with $0 < 1/\alpha \leq 1$, $0 < 1/\beta \leq 1$, $0 < 1/\gamma \leq 1$.

It should be noted that ellipsoids are important for several reasons. First, ellipsoids approximate, up to the second order, any continuous convex surface. Second, very common

surfaces, such as spheres, cylinders, and planes, can be regarded as limiting cases of an ellipsoid. Finally, the ellipsoid assumption is standard in contact mechanics (e.g. the Hertzian theory of elastic contact).

Substituting equation 9 into equation 4 yields

$$\mathbf{n} = \frac{\mathbf{A}^2\mathbf{c}}{\|\mathbf{A}^2\mathbf{c}\|} \propto \mathbf{q} = K\mathbf{A}^2\mathbf{c}, \tag{10}$$

and substituting this and equation 2 in equation 3, we obtain

$$\mathbf{m} = K\mathbf{A}^2\mathbf{r} + \mathbf{r} \times \mathbf{f}. \tag{11}$$

Equations 9 and 11 form a system of four non-linear equations and four unknowns which can be rewritten in the form

$$\boldsymbol{\Gamma}\mathbf{c} = \mathbf{m} \tag{12}$$

$$\mathbf{c}^T\mathbf{A}^2\mathbf{c} = R^2, \tag{13}$$

where $\boldsymbol{\Gamma} = \boldsymbol{\Gamma}(K)$ is a 3×3 matrix whose elements are functions of K and of the measured force components f_1, f_2 and f_3,

$$\boldsymbol{\Gamma}(K) = \begin{pmatrix} K/\alpha^2 & f_3 & -f_2 \\ -f_3 & K/\beta^2 & f_1 \\ f_2 & -f_1 & K/\gamma^2 \end{pmatrix}.$$

The determinant of $\boldsymbol{\Gamma}(K)$ is given by

$$\det \boldsymbol{\Gamma}(K) = K(K^2D^2 + \|\mathbf{A}\mathbf{f}\|^2),$$

where $D = \det \mathbf{A}$. The matrix $\boldsymbol{\Gamma}(K)$ is singular for $K = 0$, i.e. when the local torque $\mathbf{q}$ is zero. In this case (which can be detected by the simple equivalent condition $\mathbf{f}^T\mathbf{m} = 0$, as already mentioned), the contact centroid can be determined exactly by the wrench-axis method. The value of the parameter λ in equation 5 corresponding to the intersection of the wrench-axis with the ellipsoid surface is given by

$$\lambda = \frac{-\mathbf{f}'^T\mathbf{r}'_0 - \sqrt{(\mathbf{f}'^T\mathbf{r}'_0)^2 - \|\mathbf{f}'\|^2(\|\mathbf{r}'_0\|^2 - R^2)}}{\|\mathbf{f}'\|^2},$$

where $\mathbf{f}' = \mathbf{A}\mathbf{f}$ and $\mathbf{r}'_0 = \mathbf{A}\mathbf{r}_0$ (recall the definition of $\mathbf{r}_0$ in equation 6).

Whenever $\mathbf{f}^T\mathbf{m} \neq 0$, $\boldsymbol{\Gamma}(K)$ has an inverse $\boldsymbol{\Gamma}^{-1}(K)$ such that, by solving equation 12 for $\mathbf{c}$, we obtain

$$\mathbf{c} = \mathbf{\Gamma}^{-1}\mathbf{m} = \frac{1}{\det \mathbf{\Gamma}}[K^2 D^2 \mathbf{A}^{-2}\mathbf{m} + K(\mathbf{A}^2\mathbf{f}) \times \mathbf{m} + (\mathbf{f}^T\mathbf{m})\mathbf{f}]. \tag{14}$$

By substituting equation 14 into equation 13, a scalar equation in the only unknown, K, is obtained as

$$\mathbf{c}^T\mathbf{A}^2\mathbf{c} = R^2 = \frac{K^4 D^4 \|\mathbf{A}^{-1}\mathbf{m}\|^2 + K^2\|\mathbf{A}(\mathbf{A}^2\mathbf{f} \times \mathbf{m})\|^2 + (\mathbf{f}^T\mathbf{m})^2(\|\mathbf{A}\mathbf{f}\|^2 + 2K^2D^2)}{K^2(K^2D^2 + \|\mathbf{A}\mathbf{f}\|^2)^2}. \tag{15}$$

For such a 6-th order equation a closed-form solution should not be expected in general, due to Galois' theorem. For the particular surface assumed, though, we observe that

$$\|\mathbf{A}(\mathbf{A}^2\mathbf{f} \times \mathbf{m})\|^2 = D^2\left[\|\mathbf{A}^{-1}\mathbf{m}\|^2\|\mathbf{A}\mathbf{f}\|^2 - (\mathbf{f}^T\mathbf{m})^2\right],$$

so that equation 15 can be simplified in a biquadratic equation as

$$K^4D^2R^2 + K^2\left[R^2\|\mathbf{A}\mathbf{f}\|^2 - D^2\|\mathbf{A}^{-1}\mathbf{m}\|^2\right] - (\mathbf{f}^T\mathbf{m})^2 = 0.$$

Only one of the four possible K solving this equation is real and consistent with the hypothesis of non-adhesive contact, and is given by

$$K = \frac{-\text{sign}(\mathbf{f}^T\mathbf{m})}{\sqrt{2}RD}\sqrt{\sigma + \sqrt{\sigma^2 + 4D^2R^2(\mathbf{f}^T\mathbf{m})^2}}, \tag{16}$$

where

$$\sigma = D^2\|\mathbf{A}^{-1}\mathbf{m}\|^2 - R^2\|\mathbf{A}\mathbf{f}\|^2,$$

and

$$\text{sign}(x) = \begin{cases} -1, & \text{for} \quad x < 0 \\ 0, & \text{for} \quad x = 0 \\ 1, & \text{for} \quad x > 0 \end{cases}$$

By substituting K back into equation 14 and equation 10, we obtain the complete solution for $\mathbf{c}$ and $\mathbf{q}$, respectively.

5.1 Particular Cases

We will now develop solutions for some particular cases of practical importance, namely the sphere, cylinder and plane.

5.1.1 Sphere

For a spherical sensor surface of radius R centered at the origin of the force/torque reference frame B, the matrix $\mathbf{A}$ equals the identity $\mathbf{I}_3$, and $D = 1$. Hence,

$$K = \frac{-\text{sign}(\mathbf{f}^T\mathbf{m})}{\sqrt{2}R}\sqrt{\sigma' + \sqrt{\sigma'^2 + 4R^2(\mathbf{f}^T\mathbf{m})^2}}.$$

where $\sigma' = \|\mathbf{m}\|^2 - R^2\|\mathbf{f}\|^2$.

The contact centroid location (for nonzero K) is given by

$$\mathbf{c} = \frac{1}{K(K^2 + \|\mathbf{f}\|^2)}\,[K^2\mathbf{m} + K\mathbf{f} \times \mathbf{m} + (\mathbf{f}^T\mathbf{m})\mathbf{f}],$$

whereas, for $K = 0$, the contact centroid is found using equation 5 with

$$\lambda = -\frac{1}{\|\mathbf{f}\|}\sqrt{R^2 - \frac{\|\mathbf{f} \times \mathbf{m}\|^2}{\|\mathbf{f}\|^4}}.$$

5.1.2 Cylinder

Consider a cylinder having the axis parallel to the z axis of the sensor frame B, and circular cross section of radius R. Such surface can be described as the limit case of an ellipsoid with characteristic matrix given by

$$\mathbf{A} = \begin{pmatrix} 1 & 0 & 0 \\ 0 & 1 & 0 \\ 0 & 0 & 1/\gamma \end{pmatrix}$$

for $\gamma \to \infty$. Applying the same limit to equation 16, we have:

$$K = \frac{-\mathbf{f}^T\mathbf{m}}{\sqrt{R^2\|\mathbf{f}^\perp\|^2 - \|\mathbf{m}''\|^2}},$$

where $\mathbf{f}^\perp = (f_1, f_2, 0)^T$ is the component of $\mathbf{f}$ normal to the cylinder axis, and $\mathbf{m}'' = (0, 0, m_3)^T$ is the component of $\mathbf{m}$ parallel to the same axis. If $K = 0$, the wrench method (equation 5) should be applied. Otherwise, the contact centroid on the cylindrical surface of the fingertip is given by:

$$\mathbf{c} = \frac{1}{K\|\mathbf{f}^\perp\|^2}\,[K^2\mathbf{m}'' + K\mathbf{f}^\perp \times \mathbf{m} + (\mathbf{f}^T\mathbf{m})\mathbf{f}].$$

5.1.3 Plane

An ellipsoid with matrix $\mathbf{A}$ of the form

$$\mathbf{A} = \begin{pmatrix} 1/\gamma & 0 & 0 \\ 0 & 1/\gamma & 0 \\ 0 & 0 & 1 \end{pmatrix}$$

degenerates, for $\gamma \to \infty$, in a couple of parallel planes perpendicular to the x axis of B, at a distance $\pm R$ from the origin. If $\mathbf{f}'' = (0, 0, f_3)^T$ is the contact force component parallel the z axis, equations 16 and 14 become

$$K = \frac{-\mathbf{f}^T\mathbf{m}}{R\|\mathbf{f}''\|}$$

and

$$\mathbf{c} = \frac{1}{\|\mathbf{f}''\|^2}\,(\mathbf{f}'' \times \mathbf{m} + R\,\|\mathbf{f}''\|\,\mathbf{f}).$$

It should be noted that the last formula holds even with $K = 0$.

6 Iterative solution

The final method for solving the contact sensing problem is valid for any surface specification, but requires an iterative algorithm to be used at each sensor sampling time. The computational efficiency of the algorithm is therefore of utmost importance for real-time applications.

As customary when dealing with the numerical solution of vector multivariate functions, we rewrite the problem equations in the relaxation-method form

$$\mathbf{g}(\mathbf{x}) = 0, \tag{17}$$

where:

$$\begin{aligned} \mathbf{x}^T &= (x_1, x_2, x_3, x_4)^T = (\mathbf{c}^T, K/2); \\ \mathbf{g}^T(\mathbf{x}) &= (g_1(\mathbf{x}), g_2(\mathbf{x}), g_3(\mathbf{x}), g_4(\mathbf{x}))^T, \\ g_1(\mathbf{x}) &= x_4 \nabla S_1 - f_2 x_3 + f_3 x_2 - m_1; \\ g_2(\mathbf{x}) &= x_4 \nabla S_2 - f_3 x_1 + f_1 x_3 - m_2; \\ g_3(\mathbf{x}) &= x_4 \nabla S_3 - f_1 x_2 + f_2 x_1 - m_3; \\ g_4(\mathbf{x}) &= S(x_1, x_2, x_3). \end{aligned}$$

Standard algorithms (see e.g. [Dahlquist and Björk, 1974]) for the iterative solution of such equations can be applied, perhaps the most notable being the Newton-Raphson method or its variations. The Jacobian matrix $\mathbf{G}$ associated with the problem can be evaluated as

$$\mathbf{G}(\mathbf{x}) = \frac{\partial \mathbf{g}}{\partial \mathbf{x}} = \left(\begin{array}{c|c} x_4\mathbf{H} - \mathbf{f}_\otimes & \nabla S \\ \hline \nabla S^T & 0 \end{array} \right),$$

where $\mathbf{H}$ is the Hessian of the surface S (that is, the matrix $H_{ij} = \frac{\partial^2 S}{\partial x_i \partial x_j}$ $i,j = 1,2,3;$), and $\mathbf{f}_\otimes$ is the cross-product matrix of $\mathbf{f}$, such that $\mathbf{f}_\otimes \mathbf{c} = \mathbf{f} \times \mathbf{c}$.

Computing $\mathbf{G}$ can be more or less time consuming, depending upon the complexity of the surface S. Computing $\mathbf{G^{-1}}$, as required by the Newton-Raphson method, can be inconvenient for real time applications. Furthermore, in this specific case, we have that $\mathbf{G}$ is singular for $x_4 = K/2 = 0$, that means that this algorithm would present serious problems whenever the contact load has very little local torque $\mathbf{q}$.

It must be noted that, in general, the numerical solution of vector multivariate nonlinear equations is not a "nice" problem (see the related comments in [Press et al., 1988]); better algorithms are available for finding the extrema of multivariate scalar functions. A possible approach to the design of an algorithm for solving equation 17 is therefore to embed the root-finding problem in a minimization one.

Since the Jacobian matrix $\mathbf{G}$ is not symmetric (its upper left minor is the sum of a symmetric and a skew-symmetric matrix), $\mathbf{g}$ cannot be simply regarded as the gradient of some energy-like function to minimize. However, if we consider the equation

$$\mathbf{G}^T\mathbf{g}(\mathbf{x}) = 0,$$

we have that all the zeroes of $\mathbf{g}$ are also zeroes of $\mathbf{G}^T\mathbf{g}$, and $\mathbf{G}^T\mathbf{g}$ is the gradient ("potential field") associated with the positive definite scalar function $V = \frac{1}{2}\mathbf{g}^T\mathbf{g}$, whose absolute minimum is our solution.

Applying the well-known gradient descent updating law to the k-th estimate of $\mathbf{x}$, we have

$$\mathbf{x}_{(k+1)} = \mathbf{x}_{(k)} - \lambda \nabla V(\mathbf{x}) = \mathbf{x}_{(k)} - \lambda \mathbf{G}^T_{(k)}\mathbf{g}_{(k)}.$$

We observe that the application of this gradient descent technique to minimize an energy-like (Liapunov) function $V = \phi^T(\mathbf{q})\phi(\mathbf{q})$ is equivalent to the closed-loop inverse kinematic scheme proposed by Balestrino, DeMaria and Sciavicco [1984] and several others, to invert the nonlinear kinematic relationship of a robot, $\phi(\mathbf{q})$. It can be shown with a Liapunov argument that this method is locally asymptotically convergent to the desired solution, for appropriate choices of λ; and, in fact, it is intuitive that for λ (i.e. step lengths) short enough in the steepest descent direction the V function will be always kept decreasing until a minimum is reached. A discussion on the optimal choice of λ has been provided by Das, Slotine and Sheridan [1989].

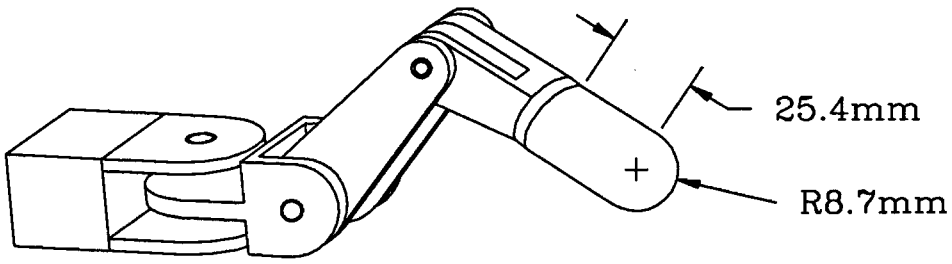

Figure 5: The fingertip sensors of the Salisbury Robot Hand are composed of a hemisphere joined to a cylinder.

The local asymptotic convergence of the algorithm means, in our current application, that the correct contact point will be found provided that the initial guess is "close enough". In order to avoid that for arbitrary initial guesses and for some force/torque readings $\mathbf{f}$, $\mathbf{m}$, the algorithm gets "stuck" at some point that does not solve the problem, it would be desirable to assess a more general global asymptotic convergence. Unfortunately, the technique of embedding the root-finding problem in a minimization one is prone to generate such local minima, and some do exist in our specific problem even for surfaces as simple as spheres. From a practical point of view those "false" roots are easily recognized (their residues $\mathbf{g}^T\mathbf{g}$ are not zero). Moreover, if the algorithm is used to continuously track a contact which changes its position and force components with continuity (i.e. it is rolling or sliding across the sensor), starting the search from the previously obtained solution is very likely to lead to the actual solution.

7 Compound surfaces

Many applications of intrinsic contact sensing use surfaces more complex than the simple geometries described above. However, the methods presented above can be extended easily to compound surfaces made of simpler surfaces if the compound surface is convex and the component surfaces share the same normal at their boundaries. For example, the fingertip sensors of the Salisbury Robot Hand are composed of a hemisphere joined to a cylinder of equal radius, as depicted in figure 5. A solution for a compound surface is typically found by trial and error: the contact centroids corresponding to the given load and to the complete ellipsoids to which the basic patches of the compound surface belong, are calculated in succession; by virtue of the uniqueness property of contact centroids, the search can be stopped as soon as a contact centroid lying on the actual sensor surface is found.

If the sensor surface has sharp points, as the example depicted in figure 6, a normal direction cannot be defined at those points and the above discussed solution methods are

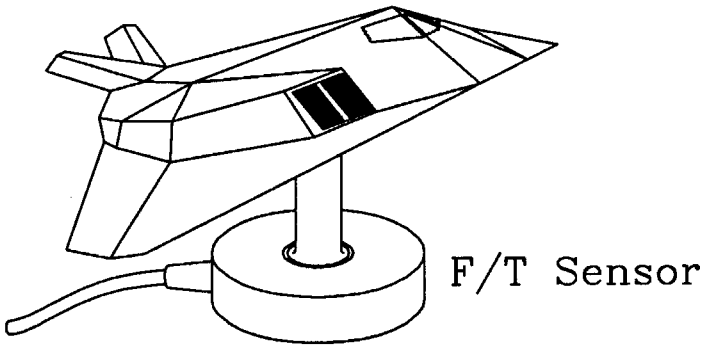

Figure 6: A compound sensor surface with corners and edges.

not applicable directly. If the sensor or the object surfaces are compliant, this problem is not a major concern, since surface edges are "smoothed" out, and the properties of the contact centroid guarantee that a meaningful result will be achieved anyway. However, if a rigid contact occurs on a sharp point of the sensor surface, no local torque is exerted; therefore, any point found by intersecting the wrench axis with the different surface patches should coincide with the actual contact point. Since, in general, only noisy measurements are available, it may happen that no contact centroid actually lying on the sensor surface is found. In this case, a good approximation can be assumed to be the point on the sensor surface closest to the calculated centroids. The worst case is when a whole edge of the sensor surface is in contact with the object. Since local torques can be exerted, and no normal direction is defined, both methods discussed above would fail. However, the practical relevance of such cases is negligible.

More complex surfaces that do not comply with the above assumptions of convexity and regularity can be dealt with in some cases. For example, a typical manipulator arm is composed of individually convex surfaces, but is not convex as a whole (see figure 7). Eberman and Salisbury [1989] discussed the use of joint torque measurements to infer information about contacts occurring on the last link of the robot. On the other hand, a force/torque sensor at the base of the manipulator would sense contacts on any link, but would not be able to distinguish among them. By the use of both base force/torque sensing and joint torque sensing it is conceivable to realize a fully sensorized robot surface. A "whole hand" manipulation system, employing intrinsic contact sensors in each phalanx of its three fingers and in the palm, has been designed, and a prototype finger built, as reported by Vassura and Bicchi [1989].

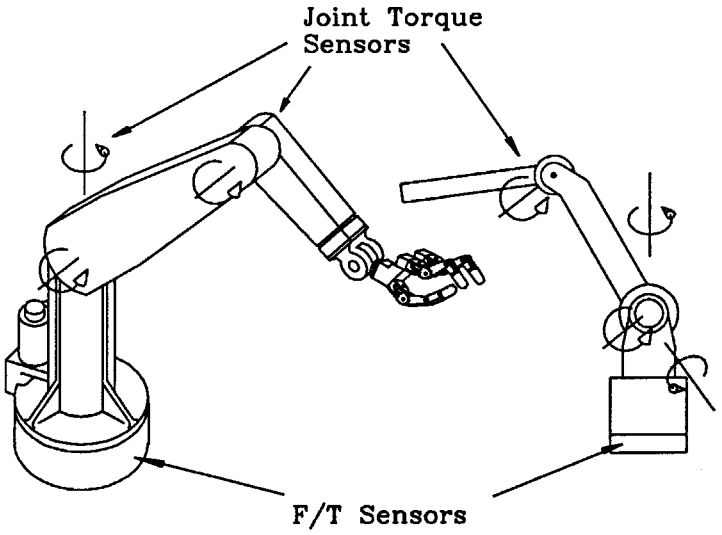

Figure 7: Fully-sensorized robot arm can be constructed in principle using only force/torque measurements.

8 Discussion and Numerical Results

In this paper we presented material on the mathematics and mechanics of intrinsic contact sensing. The paper's main contributions are perhaps the introduction of the concept of contact centroid along with the proof of its geometric properties, and the presentation of mathematical methods for computing its location on a sensor surface. In this section we will briefly elaborate on these themes, to underscore some interesting aspects.

The interest of the contact centroid for characterizing soft fingers contacts follows from its property of being located inside the convex hull enclosing every contact point. To illustrate this, a simple numerical example will be worked out. Assume that the real pattern of contact on the surface of a spherical sensor is comprised of only four points $\mathbf{c}_1, \ldots, \mathbf{c}_4$, located on top of the sphere as shown in figure 8, and let $\pm\delta$ and $\pm 8\delta$ be the coordinates along the x-axis of points $\mathbf{c}_1$, $\mathbf{c}_3$, $\mathbf{c}_2$, and $\mathbf{c}_4$ respectively.

Let the local contact forces exerted at these points be $\mathbf{h}_1 = (-h_f, h_f, -1)$, $\mathbf{h}_2 = (-h_f, h_f, -1)$, $\mathbf{h}_3 = (h_f, h_f, -1)$, and $\mathbf{h}_4 = (h_f, h_f, -1)$, respectively. Table 1 gives the x-coordinates of the contact centroid $\mathbf{c}$ (calculated through the algorithm proposed in section 5) and of the point-contact method point $\mathbf{c}'$ (section 4) corresponding to different values of δ and h_f.

As can be seen, the two results diverge as the distance δ and the friction force h_f increase. Note also that for large values of δ the contact centroid retains the characteristic of remaining

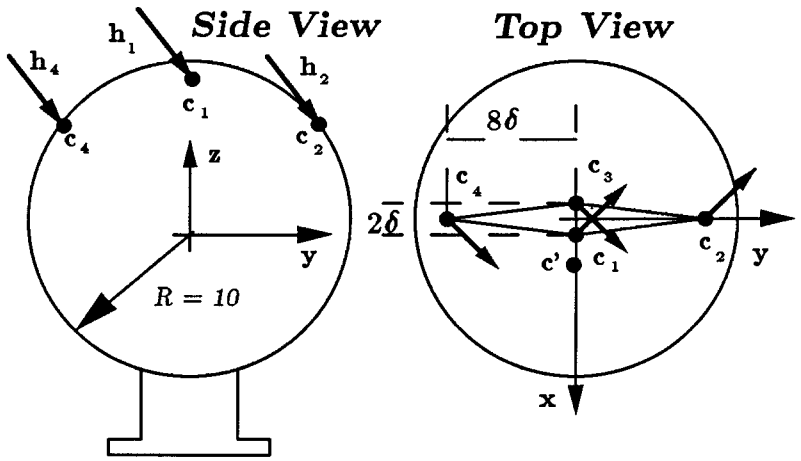

Figure 8: A simple contact pattern used as an example.

δ / h_f	0.125	0.25	0.5
0.1	c_x : 0.000	c_x : 0.000	c_x :0.000
	c'_x : 0.005	c'_x : 0.010	c'_x : 0.020
0.7	c_x : 0.000	c_x :0.005	c_x :0.039
	c'_x : 0.164	c'_x : 0.329	c'_x :0.658
1	c_x : 0.001	c_x :0.010	c_x :0.077
	c'_x : 0.250	c'_x : 0.500	c'_x :1.000

Table 1: Position of the contact centroid $\mathbf{c}$ and of the approximated (wrench-axis method) point $\mathbf{c}'$ along the x-axis for different values of δ and h_f.

	Wrench-Axis Method	Ellipsoid Method	Iterative Method
Execution time	232±6 μsec	486±13 μsec	473±13 μsec/step

Table 2: Computation times for the three algorithms to solve the contact problem on a sphere. The iterative method takes an average of 20 steps to converge under to an error of less than one part in 10^6 error when input data are slowly varying.

inside the contact points, while the point obtained by the point-contact method does not.

Another important advantage of the intrinsic contact sensing method is its ability to calculate the local torque originated from friction forces. The importance of these local torques in fine manipulation operations by robot hands has been often underestimated. To appreciate their role, consider how humans can hold a stick horizontally by pinching it at one end between two fingertips (with a gripping force of 10N, the fingers can typically resist a torque of 40Nmm and a vertical weight of 5N).

The computational efficiency of the solution algorithms is of paramount importance in real-time applications of intrinsic contact sensing. In table 2 we report computation times for the same surface, a sphere centered in the origin. The algorithms described in section4, 5 and 6 have been implemented and timed in a real-time environment running on a Motorola 68030 processor with a Motorola 68881 numeric coprocessor. Note that the iterative algorithm is inferior to the other solutions, which are both fast enough to be claimed real-time. Another weakness of the iterative method is that the multiple solutions of equation 17 cannot be discriminated in advance of their actual computation. The iterative algorithm is then recommended only for finding a complete solution for non-ellipsoidal surfaces (e.g. paraboloids) for which closed-form exact methods are not available.

To conclude the comparative analysis of the proposed algorithms, it must be noted that the exact method of section 5 is also preferable to the wrench-axis algorithm from a numerical stability point of view. In fact, as the formulation of the problem in terms of minimization of a quadratic error function given in section 6 shows, the contact problem is intrinsically stable. This is not true of the approximation that disregards local torques. Table 3 shows how small perturbations on the inputs (the force/torque sensor readings $\mathbf{f}$ and $\mathbf{m}$) reflect in small perturbation in the calculated contact point for the method of section 5, while they can lead to inconsistent (complex) results for the wrench-axis method.

Devices based on the force-based contact sensing approach have been actually implemented, and effectively employed in robotic hands. For a discussion on the realization of force/torque sensors on small robot fingertips, see [Brock and Chiu, 1985], and [Bicchi 1987]. The latter paper discusses the application of optimal design techniques to miniaturized force/torque sensors; this approach is expanded in a more thorough treatment in

Method F/T Measurements	Wrench-Axis	Ellipsoid	Iterative
f = [-0.3 -.04 0.01] **m** = [0.01 0.01 0.48]	**c**′ = [-0.60 0.80 0.00]	**c** = [-0.60 0.80 0.00]	**c** = [-0.60 0.80 0.00]
f = [-0.3 -.04 0.01] **m** = [0.01 0.01 0.49]	**c**′ = [-0.66 0.75 0.00]	**c** = [-0.66 0.75 0.04]	**c** = [-0.66 0.75 0.04]
f = [-0.3 -.04 0.01] **m** = [0.01 0.01 0.50]	**c**′ = [? ? ?]	**c** = [-0.74 0.67 0.09]	**c** = [-0.73 0.68 0.07]
f = [-0.3 -.04 0.01] **m** = [0.01 0.01 0.51]	**c**′ = [? ? ?]	**c** = [-0.76 0.62 0.20]	**c** = [-0.76 0.62 0.20]

Table 3: Algorithm sensitivity example. Noise on the measurement of the second component of the measured moment **m** is simulated. The centroid is computed for a unit radius sphere. Question marks indicate inconsistent (complex) results.

[Bicchi,1990b].

The applications of intrinsic contact sensors to robotic manipulation are numerous, and several have been experimentally verified. Although it is not possible to detail these applications here, they will be cited for reference:

- The exploration of unknown objects by probing with an intrinsic tactile sensor, and the reconstruction of their surface profile has been described by Brock and Chiu [1985], and later by Tsujimura and Yabuta [1988]. Both authors employed the point-contact method algorithm. Bicchi [1989] reported explorations performed using the more precise algorithm of section 5, and an hybrid control scheme, which allowed continuous control of the normal component of contact force.

- The capability of intrinsic contact sensors to evaluate the friction components of the contact force and the local torque (which is unique among other available sensing devices), has been used to measure the coefficients of friction of various objects [Bicchi, 1989]. This information in turn has been used to discriminate between objects on the basis of their apparent friction, and to plan subsequent slippage-safe operations of the hand.

- A real-time control method for augmenting the stability of the grasp of unmodeled objects against slippage has been discussed and demonstrated (in a rather simple setting) by Bicchi, Salisbury and Dario [1989].

The exploitation of contact sensory information is expected to allow improvements in many areas of fine manipulation control. Contact sensors such as those described in this

paper can provide direct, real-time and reliable feedback of fundamental contact interaction characteristics. For instance, intrinsic contact sensors could be profitably used to improve the accuracy of the control of micro-motions of manipulated objects or tools, especially in the presence of slipping and/or rolling contacts.

References

Balestrino, A., De Maria, G., and Sciavicco, L. "Robust Control of Robotic Manipulators," Proceedings of the 9th IFAC World Congress, vol.6, pp. 80-85, 1984.

Bicchi, A., "Strumenti e Metodi per il Controllo di Mani per Robot," PhD Thesis, Università di Bologna, 1989.

Bicchi, A.: "Intrinsic Contact Sensing for Soft Fingers," Proc. IEEE Int. Conf. Robotics and Automation, Cincinnati, OH, May 1990.

Bicchi, A. "A Criterion for the Optimal Design of Multi-Axis Force Sensors," MIT AI Lab Memo 1263, 1990b.

Bicchi, A., Dario, P., "Intrinsic Tactile Sensing for Artificial Hands," Proc. 4th Int. Symp. on Robotics Research, Santa Barbara, CA. R. Bolles and B. Roth Editors, published by the MIT Press, Cambridge, MA, 1987.

Bicchi, A., Salisbury, J.K., Dario, P. "Augmentation of Grasp Robustness Using Intrinsic Tactile Sensing," Proc. IEEE Conf. on Robotics and Automation, Scottsdale, Arizona, 1989.

Brock, D.L, and Chiu, S. "Environment Perceptions of an Articulated Robot Hand Using Contact Sensors," Proc. ASME Winter Annual Meeting, Miami, FL, 1985.

Dahlquist, G., and Björk, Å. "Numerical Methods", Prentice Hall, 1974.

Das, H., Slotine, J.-J.E., and Sheridan, T.B. "Inverse Kinematic Algorithms for Redundant Systems," Proc. IEEE Int. Conf. on Robotics and Automation, Philadelphia, 1988.

Eberman, B. S. and Salisbury, J.K.: "Determination of Manipulator Contact Information from Joint Torque Measurements", Experimental Robotics I, First International Symposium, Montréal, Canada, June 1989. Published in Lecture Notes in Control and Information Sciences, Hayward, V. and O. Khatib (Eds.), Springer-Verlag, 1990.

Hunt, K.H.: "Kinematic Geometry of Mechanisms," Oxford University Press, London, England, 1978.

Johnson, K.L. "Contact Mechanics", Cambridge University Press, 1985.

Mason, M.T. and Salisbury, J.K. "Robot Hands and the Mechanics of Manipulation," MIT Press, Cambridge, MA, 1985.

Minsky, M. "Manipulator Design Vignettes," MIT AI Lab Memo 267, 1972, re-issued as MIT AI Lab Memo 267A, 1981.

Nicholls, H.R. and Lee, M.H., "A Survey of Robot Tactile Sensing Technology," IJRR, Vol 3., No. 3., June 1989.

Okada, T.: "A New Tactile Sensor Design Based on Suspension-Shells", in *Dextrous Robot Hands*, Venkataraman, S.T., and Iberall, T., eds. Springer-Verlag, New York, NY, 1990.

Peronneau, G., "Position-Indicating System," US Patent Number 3,657,475, April 1972.

Press, W.H., Flannery, B.P., Teukolsky, S.A., Vetterling, W.T. "Numerical Recipes", Cambridge University Press, 1988.

Salisbury, J. K., "Kinematic and Force Analysis of Robot Hands," Ph.D. Thesis, Stanford University, 1982.

Salisbury, J.K., "Interpretation of Contact Geometries from Force Measurements," Proc. 1st International Symposium on Robotics Research, Bretton Woods, N.H.. M.Brady and R.Paul Editors, published by the MIT Press, Cambridge, MA, 1984.

Tsujimura, T., and Yabuta, T. "Object Detection by Tactile Sensing Method employing Force/Torque Information," IEEE Transactions on Robotics and Automation, vol.5, no.4, August 1988.

Vassura, G. and Bicchi, A.: "Whole Hand Manipulation: Design of an Articulated Hand Exploiting All Its Parts to Increase Dexterity," in Robots and Biological Systems, NATO-ASI Series, P.Dario, G.Aebischer, G.Sandini eds., Springer-Verlag, Berlin, RFG, 1989.

Whitney, D.E. "Historical Perspective and State of the Art in Robot Force Control," International Journal of Robotic Research, Vol. 6, No. 1, Spring 1987.

Appendix 1.

The contact centroid general property (Proposition 1) given in section 2.1 will be proved in three steps, where properties of increasing generality are illustrated:

Property 1: If a distribution Δ of compressive contact tractions $\mathbf{v}(\mathbf{r})$, acts on a set of contact points $C = \{\mathbf{r}_c\}$ of a planar surface $P(\mathbf{r}) = 0$, the contact centroid of Δ on P lies inside the convex hull enclosing every point $\mathbf{r}_c$ (see figure 9).

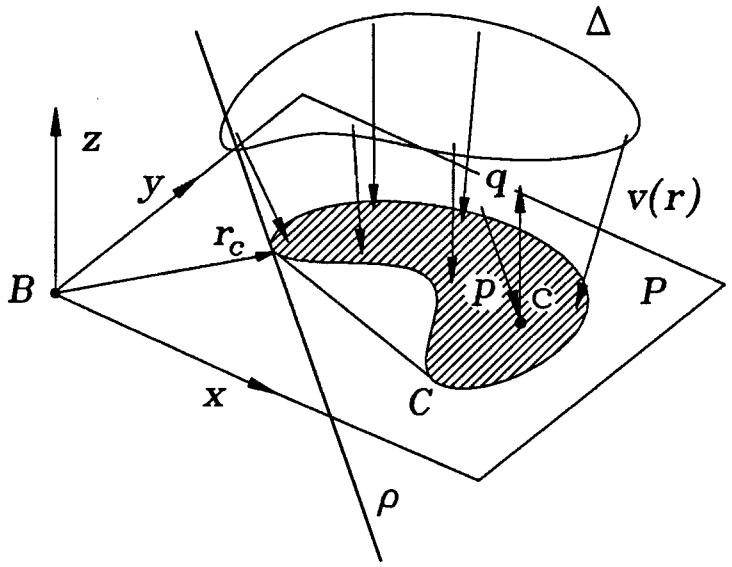

Figure 9: Contact on a planar surface.

Proof: Consider a line ρ in the contact plane P passing through at least one contact point $\mathbf{r}_c$ and leaving all others on the same half plane, as depicted in figure 9. By definition 1, a set of forces equivalent to the given contact set is comprised of a resultant force $\mathbf{p} = \int_P \mathbf{v}(\mathbf{r})$ applied at the contact centroid, and a torque $\mathbf{q}$ normal to the contact plane. In order to satisfy the balance of moments about the line ρ, the contact centroid must lie on the same half plane where the contact points do. Considering the family of all such lines ρ, the convex hull results as the envelope of the family, and the proposition follows.

In other words, for a planar sensor with compressive forces, no matter how far away the contact points are from each other, the contact can be considered 'soft finger', and the contact centroid lies inside the smallest convex polygonal line enclosing every contact point.

Property 2: Consider a convex surface $S(\mathbf{r}) = 0$ (see figure 10), and a plane $P(\mathbf{r}) = 0$ intersecting S. Let $\mathbf{n}'$ be the normal unit vector to P, pointing at the half space where $P(\mathbf{r}) > 0$). Assume that a distribution Δ of contact tractions $\mathbf{v}(\mathbf{r})$ is exerted on a set C of points $\mathbf{r}_c$ lying on P and internal to S , and assume that the tractions are compressive with respect to $\mathbf{n}'$ (i.e., $\mathbf{n}'^T\mathbf{v}(\mathbf{r}_c) < 0$, for all $\mathbf{r}_c$). In these hypotheses, the contact centroid of Δ on S lies in the half space $P(\mathbf{r}) > 0$.

Proof: Because of the first property of contact centroids, the distribution Δ of contact forces applied on C is equivalent to its resultant force $\mathbf{p}$ applied to a contact centroid $\mathbf{c}'$ on P, and torque $\mathbf{q}'$, such that $\mathbf{c}'$ is inside S and $\mathbf{q}'$ is parallel to $\mathbf{n}'$. We denote with $\mathbf{c}$, $\mathbf{n}$ and $\mathbf{q}$ the contact centroid of Δ on S, the associated normal, and the local torque, respectively. Let moreover $\mathbf{e} = \mathbf{c} - \mathbf{c}'$. The balance of moments about $\mathbf{c}'$ can then be written as

$$\mathbf{q}' = \mathbf{q} + \mathbf{e} \times \mathbf{p}, \tag{18}$$

which can be rewritten as:

$$\xi'\mathbf{n}' = \xi\mathbf{n} + \mathbf{e} \times \mathbf{p}, \tag{19}$$

where ξ and ξ' are scalar constants. By multiplying both members of equation 19 by $\mathbf{p}^T$, and by $\mathbf{e}^T$, we obtain two equations:

$$\xi'\mathbf{p}^T\mathbf{n}' = \xi\mathbf{p}^T\mathbf{n}, \tag{20}$$
$$\xi'\mathbf{e}^T\mathbf{n}' = \xi\mathbf{e}^T\mathbf{n}, \tag{21}$$

For the hypotheses above and for the definition of contact centroid, $\mathbf{p}^T\mathbf{n}' < 0$ and $\mathbf{p}^T\mathbf{n} < 0$ (compressive contact). Hence, from equation 20, ξ and ξ' must have the same sign or be both zero.

If ξ and ξ' are not null and have the same sign, from equation 21 follows that also $\mathbf{e}^T\mathbf{n}'$ and $\mathbf{e}^T\mathbf{n}$ have the same sign. Since S is convex and $\mathbf{c}'$ is inside S, $\mathbf{e}^T\mathbf{n} > 0$ for every $\mathbf{e}$. Therefore, $\mathbf{e}^T\mathbf{n}' > 0$, that is $\mathbf{e}$ points to the half space $P(\mathbf{r}) > 0$ as required.

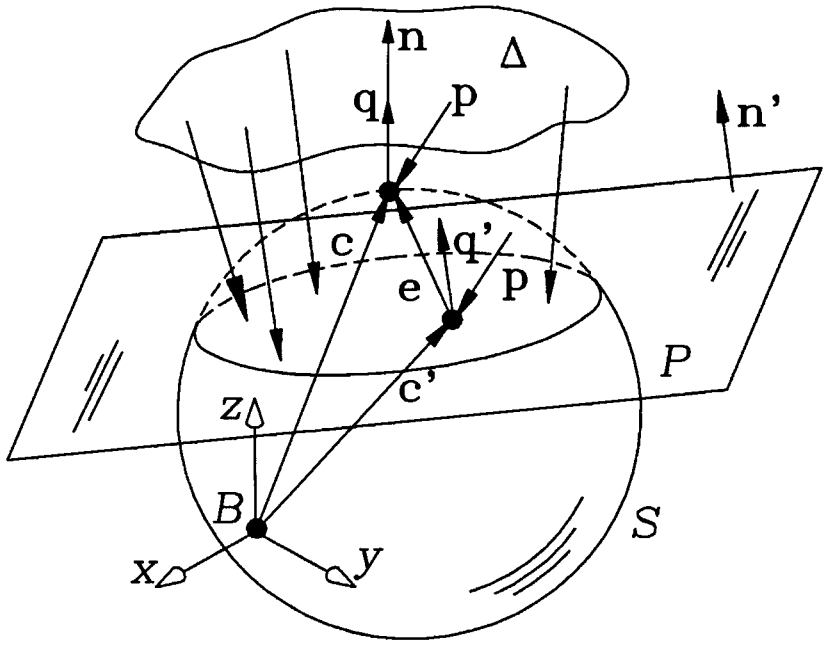

Figure 10: Contact on a deformable surface.

Otherwise, if both ξ and ξ' are zero, than from equation 19 follows that $\mathbf{e}$ and $\mathbf{p}$ must be parallel. Let then $\mathbf{e} = \zeta\mathbf{p}$; using again the fact that $\mathbf{p}^T\mathbf{n} < 0$ (definition of contact centroid) and that $\mathbf{e}^T\mathbf{n} = \zeta\mathbf{p}^T\mathbf{n} > 0$ (convexity of S), we have that $\zeta < 0$. Since also $\mathbf{c}'$ is a contact centroid, $\mathbf{p}^T\mathbf{n}' < 0$. Finally we have then $\mathbf{e}^T\mathbf{n}' = \zeta\mathbf{p}^T\mathbf{n}' > 0$, q.e.d..

Rephrased, this second property has intuitive meaning. Consider a sensor with convex, compliant surface which is deformed by contact with a flat object: no adhesive forces are exerted, and the deformed surface stays inside the undeformed one. Since the deformed surface is not known, the contact centroid can only be calculated relative to the sensor undeformed surface. However, the contact centroid is well behaved, in the sense that it will stay on the same side of the areas being touched (see figure 10).

Property 3: Consider a deformable body, whose undeformed surface $S(\mathbf{r}) = 0$ is convex, and assume that a distribution Δ of compressive contact tractions is exerted on a set of contact points $C = \{\mathbf{r}_c\}$ of S. Consider a plane $P(\mathbf{r}) = 0$ that divides the surface of the deformed body in two portions, so that every contact point is confined in one half-space (see figure 2). Consider the projection of each contact point $\mathbf{r}_c$ on P along the direction of the traction applied at $\mathbf{r}_c$: if all such

projections lie inside the undeformed surface S, then the contact centroid on S of Δ lies on the same side of P where Δ is applied.

Proof: Since pure forces or tractions can be moved along their line of application without affecting the resultant force and torque of the set, this proposition is easily derived from property 2.

In order to give the best estimate of the location of contact points, the plane P can be chosen as the one that separates the smallest portion of S enclosing every contact point/area; if some contact points belong to P, it is required that the contact traction at those points be strictly compressive with respect to the plane.

Appendix 2.

Proposition 2: Uniqueness of Solutions

A solution to the contact sensing problem, described by equations 1 through 4 and by the definition of contact centroid, is unique (if it exists), if and only if the surface is convex.

Proof: The "if" part of the proposition can be demonstrated by contradiction: assume that there are two points, $\mathbf{c}$ and $\mathbf{c}'$ (expressed in an arbitrary reference frame B) lying on a convex surface S, that are solutions of the contact sensing problem, and consider the vector $\mathbf{e} = \mathbf{c}' - \mathbf{c}$ (see figure 11). Because of the surface convexity we have that:

$$\begin{aligned} \mathbf{e}^T\mathbf{n}' &> 0, \\ \mathbf{e}^T\mathbf{n} &< 0. \end{aligned} \tag{22}$$

The balance of moments at point $\mathbf{c}$ can be written as

$$\mathbf{q} = \mathbf{q}' + \mathbf{e} \times \mathbf{p},$$

Since $\mathbf{q}$ and $\mathbf{q}'$ are parallel to $\mathbf{n}$ and $\mathbf{n}'$ respectively, we can rewrite

$$\xi\mathbf{n} = \xi'\mathbf{n}' + \mathbf{e} \times \mathbf{p}, \tag{23}$$

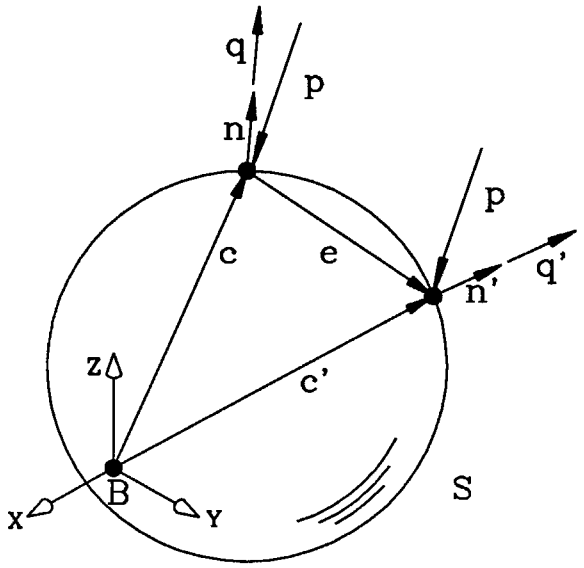

Figure 11: The contact centroid on a convex surface is unique.

and, by multiplying both terms by $\mathbf{p}^T$, we have

$$\xi \mathbf{p}^T \mathbf{n} = \xi' \mathbf{p}^T \mathbf{n}',$$

which, since forces are assumed compressive, implies that either $\xi\xi' > 0$ or $\xi = \xi' = 0$.

If $\xi = \xi' = 0$, no local torques are exerted at $\mathbf{c}$ nor at $\mathbf{c}'$, and those points lie on a line parallel to $\mathbf{p}$. Because of the convexity of S, only one of the two intersections of such line can satisfy the definition of contact centroid ($\mathbf{p}^T\mathbf{n} < 0$).

If $\xi\xi' > 0$, by multiplying both terms of equation 23 by $\mathbf{e}^T$, we obtain

$$\xi \mathbf{e}^T \mathbf{n} = \xi' \mathbf{e}^T \mathbf{n}',$$

that, together with the convexity condition 22, implies either $\xi\xi' < 0$ (a contradiction), or $\mathbf{e} = 0$, the proposition. In addition, it can be easily shown that the uniqueness of the contact centroid holds also if the surface is planar, provided that the contact tractions are strictly compressive.

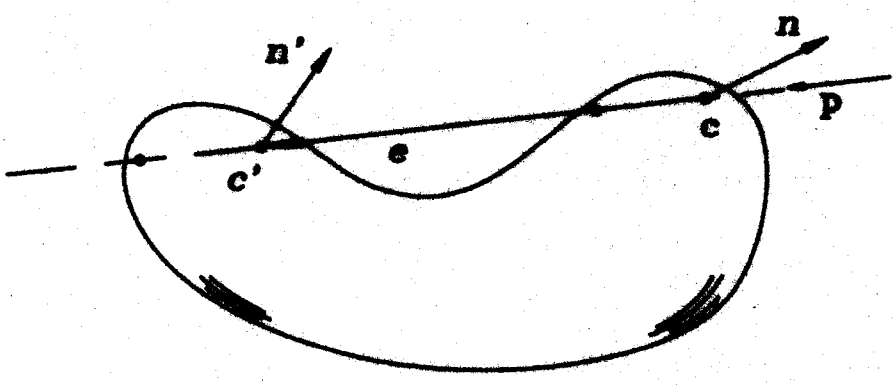

Figure 12: Concave surfaces may have non-unique contact centroids

To demonstrate the "only if" part, suppose the surface is not convex; that is, there exist two distinct points such that

$$\begin{aligned} \mathbf{e}^T\mathbf{n}' &< 0, \\ \mathbf{e}^T\mathbf{n} &< 0. \end{aligned} \tag{24}$$

Thus a compressive force in the direction of e applied at either point yields identical sets of forces and moments. Hence the solution is not unique and the statement is proved.

This blank page was inserted to preserve pagination.

REPORT DOCUMENTATION PAGE

Form Approved
OMB No. 0704-0188

1. AGENCY USE ONLY (Leave blank)	2. REPORT DATE	3. REPORT TYPE AND DATES COVERED
	October 1990	memo

4. TITLE AND SUBTITLE
Contact Sensing from Force Measurements

5. FUNDING NUMBERS
N00014-86-K-0685
NAG-9-319

6. AUTHOR(S)
Antonio Bicchi
J. Kenneth Salisbury
David L. Brock

7. PERFORMING ORGANIZATION NAME(S) AND ADDRESS(ES)
Artificial Intelligence Laboratory
545 Technology Square
Cambridge, Massachusetts 02139

8. PERFORMING ORGANIZATION REPORT NUMBER
AIM 1262

9. SPONSORING/MONITORING AGENCY NAME(S) AND ADDRESS(ES)
Office of Naval Research
Information Systems
Arlington, Virginia 22217

10. SPONSORING/MONITORING AGENCY REPORT NUMBER
AD-A234387

11. SUPPLEMENTARY NOTES
None

12a. DISTRIBUTION/AVAILABILITY STATEMENT
Distribution of this document is unlimited

12b. DISTRIBUTION CODE

13. ABSTRACT *(Maximum 200 words)*

This paper addresses contact sensing, i.e. the problem of resolving the location of a contact, the force at the interface and the moment about the contact normals. Called "intrinsic" contact sensing for the use of internal force and torque measurements, this method allows for practical devices which provide simple, relevant contact information in practical robotic applications. Such sensors have been used in conjunction with robot hands to identify objects, determine surface friction, detect slip, augment grasp stability, measure object mass, probe surfaces, control collision and a variety of other useful tasks. This paper describes the theoretical basis for their operation and provides a framework for future device design.

14. SUBJECT TERMS (key words)
Contact Sensing
Contact Mechanics
Dextrous Manipulation

15. NUMBER OF PAGES
31

16. PRICE CODE
$4.00

17. SECURITY CLASSIFICATION OF REPORT	18. SECURITY CLASSIFICATION OF THIS PAGE	19. SECURITY CLASSIFICATION OF ABSTRACT	20. LIMITATION OF ABSTRACT
UNCLASSIFIED	UNCLASSIFIED	UNCLASSIFIED	UNCLASSIFIED

CS-TR Scanning Project
Document Control Form

Date : 10/17/94

Report # AIM-1262

Each of the following should be identified by a checkmark:
Originating Department:

☒ Artificial Intellegence Laboratory (AI)
☐ Laboratory for Computer Science (LCS)

Document Type:

☐ Technical Report (TR) ☒ Technical Memo (TM)
☐ Other:_____

Document Information

Number of pages: 31
Not to include DOD forms, printer intstructions, etc... original pages only.

Originals are:
☒ Single-sided or
☐ Double-sided

Intended to be printed as :
☐ Single-sided or
☒ Double-sided

Print type:
☐ Typewriter ☐ Offset Press ☒ Laser Print
☐ InkJet Printer ☐ Unknown ☐ Other:_____

Check each if included with document:

☒ DOD Form ☐ Funding Agent Form ☐ Cover Page
☐ Spine ☐ Printers Notes ☐ Photo negatives
☐ Other: _____

Page Data:

Blank Pages(by page number):_____

Photographs/Tonal Material (by page number):_____

Other (note description/page number):

Description : Page Number:

_____
_____
_____
_____

Scanning Agent Signoff:

Date Received: 10/17/94 Date Scanned: 10/18/94 Date Returned: 10/20/94

Scanning Agent Signature: Michael W. Cook